INL/EXT-15-34493
Revision 1

Progress Report on Development of Texture Measuring Technique via XRD

Leah Squires
Thomas Hartmann

March 2015

The INL is a U.S. Department of Energy National Laboratory
operated by Battelle Energy Alliance

INL/EXT-Error! Reference source not found.
Revision 1

Progress Report on Development of Texture Measuring Technique via

Leah Squires
Thomas Hartmann

March 2015

Idaho National Laboratory
Idaho Falls, Idaho 83415

http://www.inl.gov

Prepared for
TerraPower, LLC
Under CRADA 13-CR-13
And DOE Idaho Operations Office
Contract DE-AC07-05ID14517

CONTENTS

FIGURES

TABLES

Progress Report on Development of Texture Measuring Technique via

XRD-Based Texture Analysis using MULTEX 3 on Selected Samples

This review provides an overview of the results of XRD-based texture analysis using MULTEX 3 with respect to expectations for uranium-based fuel samples. In the following examples we have chosen samples with the highest possible texture (single crystal Mo) to virtually no texture (corundum powder). We will compare the results of XRD-based texture analysis of these ten samples:

1. Molybdenum single crystal
2. Rolled Copper
3. Alumina powder (corundum) pressed pellet
4. α-uranium
5. R1a2R1a5a (U10Zr)
6. R1c2R1c5a (U10Zr)
7. R2c2R2c5a (U10Zr)
8. R2a2R2a5a (U10Zr)
9. Ra2Ra5a (U10Zr)
10. U5Fs rod, where 5Fs = 2.44Mo-1.95Ru-0.3Rh-0.2Pd-0.09Zr-0.02Nb

Objective

The objective of this work is to develop an efficient technique to determine texture properties of TerraPower zirconium bearing fuel materials and micro-alloyed fuels using the Bruker D8 Discover X-ray diffractometer (XRD) currently located in the Analytical Laboratory at MFC. Experimental data on microstructure and grain orientation provide the foundation of material engineering in order to optimize fabrication. The material grain structure and grain orientation affect thermo-physical properties of reactor materials such as heat capacity, thermal conductivity, thermal diffusivity, radiation resistance, and radiation growth. Determination of texture grain structure or lack thereof is essential to understand and predict fuel properties. In order to avoid anisotropic radiation induced swelling in the fuel TerraPower has specified that fuel microstructure must be randomly oriented.

This work focused on developing an efficient method to verify random orientation in fuel samples using XRD based methods. This data will greatly enhance our understanding of how material casting and manufacturing techniques, in particular extrusion, as well as heat treatment and irradiation, change the material texture. Also this technique can be used to verify the requirement of a randomly oriented microstructure is met. In addition it will allow us to better understand how changes in the texture of a material affect its mechanical and thermo-physical properties.

Background

Texture in EBR-II type driver fuel was historically quantified using X-ray diffraction and the relative peak intensity ratios of the diffraction peaks (110) and (021) were compared as $I_{(110)}/I_{(021)}$ (Sturcken & Walter, JNM 50(1974), 69-82). X-ray diffraction studies indicated the presence of preferred orientation (texture) in these fuel pins with an increase of the peak intensity in (110) and a decrease of (021) in axial direction. Furthermore texture at the fuel pin bottom was increased compared with texture in the top region. For polycrystalline uranium, preferred orientation causes anisotropic dimensional changes during irradiation. Impact-bonded and special heat treated fuel pins had $I_{(110)}/I_{(021)}$ ratios between 0.77 and 0.8,

while centrifugally bonded pins had $I_{(110)}/I_{(210)}$ ratios between 0.96 and 1.32. Using the experimental set-up of Sturcken & Walter, a $I_{(110)}/I_{(021)}$ ratio of 0.79 represents a perfectly random orientation. However, the $I_{(110)}/I_{(021)}$ peak intensity ratio is affected by the individual instrumental set up, the axial convolution and the Lorentz polarization of the beam path. For the Bruker D8 Discover at INL a perfectly random microstructure within the α-uranium specimen is indicated by a $I_{(110)}/I_{(021)}$ ratio of 0.738(2) for relative intensities and a $I_{(110)}/I_{(021)}$ ratio of 0.702(1) for absolute peak intensities.

Refer to Table 1 for experimental set-up and its impact on peak ratio. Using this computational approach we can show that the experimental setting of the powder diffractometer very little impact on the structure amplitudes $|F_{hkl}|$ for (110) and (021) of α-uranium and therefore on the calculated absolute intensities. The absolute peak intensity ratio $I_{(110)}/I_{(021)}$ remains nearly unchanced while changing the individual parameters.

Table 1. Impact of experimental parameters on absolute peak intensity ratio.

Emis-sion	Gonio-meter	Lorentz Polarization	Detector	Receiving Slit	FDS	Source Length	VDS	Prim. Soller	Secon. Soller	Fhkl2 (110)	Fhkl2 (021)	I(110)/I(021)
Cu Ka1/Ka2	217.5 / 217.5	90	point	na	na	12 mm	na	na	na	17.165	24.502	0.70056
	217.5 / 217.5	45	point	na	na	12 mm	na	na	na	9.864	14.079	0.70062
	217.5 / 217.5	0	point	na	na	12 mm	na	2.3	na	10.641	15.19	0.70053
	217.5 / 217.5	0	point	0.1 mm	1 °	12 mm	na	2.3	na	10.641	15.175	0.70122
	217.5 / 217.5	0	point	0.1 mm	1 °	12 mm	na	2.3	2.3	10.637	15.17	0.70119
	217.5 / 217.5	0	point	0.05 mm	2 °	12 mm	na	2.3	2.3	10.64	15.175	0.70115
	217.5 / 217.5	0	point	0.1 mm	na	12 mm	12 mm	2.3	2.3	10.64	15.174	0.70120
	217.5 / 217.5	0	PSD 4° linear	na	1 °	12 mm	na	2.3	2.3	10.639	15.171	0.70127
	435 / 217.5	0	PSD 4° linear	na	1 °	12 mm	na	2.3	2.3	10.64	15.175	0.70115
	435 / 217.5	27.3	PSD 3° linear	na	5 °	12 mm	na	2.3	2.3	10.64	15.175	0.70115
	435 / 217.5	27.3	PSD 3° linear	na	1 °	1 mm	na	na	2.3	10.64	15.174	0.70120
	435 / 217.5	27.3	point	0.1 mm	1 °	1 mm Capillary	na	na	2.3	10.64	15.174	0.70120
Cu Ka1	435 / 217.5	27.3	PSD 3° linear	na	1 °	3 mm	na	2.3	2.3	10.635	15.167	0.70119
	435 / 217.5	27.3	point	0.1 mm	na	3 mm	1 mm	2.3	2.3	10.635	15.167	0.70119

Hereby the relative peak intensity ratio $I_{R(110)}/I_{R(021)}$ as applied by Sturcken & Walter is defined by the net-peak intensities as background-corrected maximum intensities (counts), while the absolute peak intensity ratio $I_{A(110)}/I_{A(021)}$ is derived by peak integration of the net-counts under the peak (Σ counts x Δ2θ) and directly represents the ratio of the squares of the structure amplitudes to be formulated as $F^2_{(110)}/F^2_{(021)}$. The latter is extracted by applying peak profile fitting and Rietveld structure refinement.

The peak ratio method by Sturcken & Water was applied on α-uranium samples with no interference of a secondary phase. The presence of γ-uranium and/or δ-UZr_2 limits the application of this methods due to the overlay of peak intensities from a second or third phase. This report describes the development of a

technique to use pole figures built from α-uranium peaks with no interference from the γ-uranium and/or δ-UZr_2 phases. A recently developed method combining Rietveld structure refinement with Pawley or Le Bail peak profile fitting to overcome this obstacle will also be touched upon briefly in this report. This method was successfully applied to determine texture in the α-uranium phase in U5Fs despite the interference with peak intensities of γ-uranium. One caveat hereby is that for all phases other than α-uranium random texture conditions have to be assumed for the new technique. Future work will include using the Rietveld structure refinement combined with the Pawley or Le Bail peak profile fitting to analyze bulk data from the archived samples and compare these results with the pole figure results.

Explanation of Representations and Key Terms

Pole Figures

A pole figure is a representation of the crystal plane normal plotted with respect to a sample frame. This sample frame is a sphere with an equatorial plane in which the crystal sits. Unit vectors from each plane of the crystal intersect the sphere and are projected through the equatorial plane to the pole of the sphere. The intersections of the unit vectors with the equatorial plane are plotted to create the pole figure. Only the upper hemisphere is plotted by convention. When measuring a polycrystalline material it is important to have more than one pole and it is necessary to bin the data and convert the points into densities which are then represented as contour plots. The figure below gives an explanation of a pole figure.

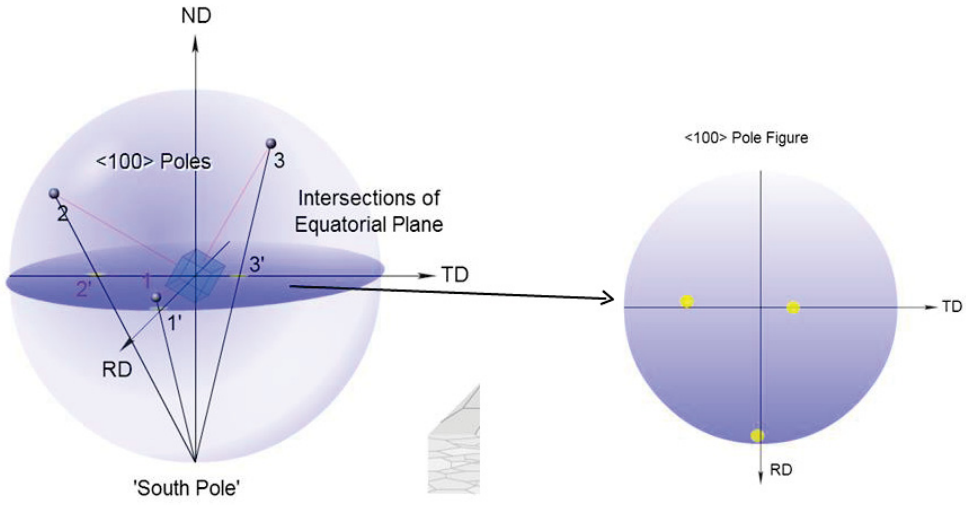

Figure 1. Schematics of pole figures.
Normal vectors from each (100) plane in the sample can be projected onto the sphere. The place where the crystallographic direction intersects with the surface of the unit sphere is a pole. The poles are then reflected through the equatorial plane to the south pole of the sphere and the point at which each resulting vector intersects the equatorial plane is represented on the2D pole figure.
NOTE: *The pole figure is in reference to ND (normal direction).*

Inverse Pole Figures

An inverse pole figure is a map of a selected set of sample directions plotted with respect to the crystal frame. In inverse pole figures three directions, the rolling direction (RD), the transverse direction (TD) and the normal direction (ND) are plotted. In our case since there is no rolling direction, the normal direction is defined as the direction axial the fuel cross section. Sample symmetry in this case is ignored because the 3 sample directions are very rarely equivalent. As with pole figures, data from polycrystalline samples is binned and displayed as contour plots (Figure 2).

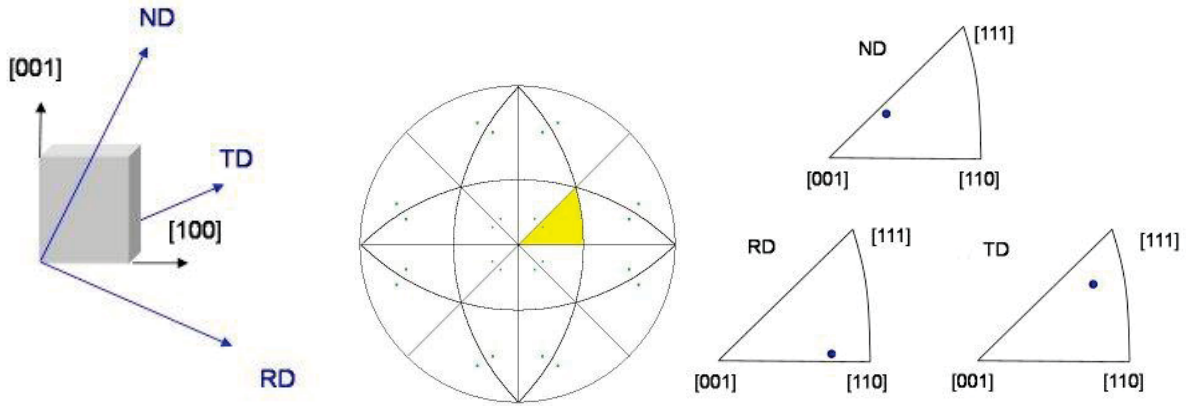

Figure 2. Schematics of inverse pole figures.
Left: In inverse pole figures the axes of the projection sphere are aligned with the crystal directions rather than the sample axis. Center: The direction parallel to the normal direction (ND) is plotted on a stereographic projection with the axes parallel to the edges of the unit cell (cubic in this case). Right: The yellow area from the center figure is used to form the ND inverse pole figure. The rolling direction (RD) and transverse direction (TD) pole figures are obtained similarly with respect to the rolling and transverse directions. (www.ebsd.com)

Multiple Intensity of Random Distribution (MRD)

The Multiple Intensity of Random Distribution (MRD) value is the normalized probability density of a given orientation. The higher this number is, the stronger the texture. The lower this number is, the weaker the texture. In this report we use the term in reference to the iso-lines as referred to in the Multex 3 user manual (3-17). Multex 3 displays contour lines similar to a topographic map and does not provide normalized MRD values. Considering near-perfect conditions (example single crystal molybdenum) with very substantial texture with diffracted intensities of narrow FWHMs, the contour lines start from 0, since all diffracted intensities are concentrated around the peaks representing the reciprocal lattice for the individual textured orientation. The contour lines are therefore a pseudo-representation of MRD values since they directly represent measured intensities and are not normalized. This normalization might be accomplished by the division of the measured peak intensities by peak intensities of random distribution, which is an integer.

The MRD or equivalent value is a common representation of preferred orientation for textured samples. The value describes the factor by which specific orientations of crystallites are over-represented compared with random condition and thus the factor by which the intensity of the reciprocal lattice of these orientations are over-represented in the diffraction patterns or the pole figures. Under ideal conditions a MRD value of 1 represents perfectly random conditions and corresponds to a contour line of 0 using the MULTEX 3 notation as shown for the case of single crystal Mo. As a result of the weak texture and near random conditions in the U10Zr samples, the orientation density of these samples cannot be resolved due to large FWHMs, and the iterations with the attempt to minimize χ^2 were only partly successful. We concluded random orientation even for pseudo-MRD values of 2-3 (Multex contour lines) since texture modelling does not converge.

Multex 3 software does *not* precisely apply MRD values but iso-lines, which are similar to contour lines of topographic maps. In the case of no texture, the measured pattern does not have any contour lines other than 0, since no orientation of the reciprocal lattice is over-represented. For significant texture, the intensity of the reciprocal lattice for the individual crystallographic orientation in the diffraction pattern, the so-called pole figure, is significantly higher than the pattern calculated for random condition, and the pole figure shows 2-dimesional peaks of ideally rather narrow shape with small full width at half maximum (FWHM) values above background (iso-line 0). The calculated pole intensities should be at

least 2-3 iso-lines above background. The pole figures for each orientation are defined by the Laue class of the material (*mmm* for α-uranium, *m-3m* for γ-uranium) but also by the sample history and its treatment e.g. by cold working (forging or rolling).

The U-10Zr fuel alloys do show rather insignificant texture (cold working history is lacking) which is derived by the fact of blurry pole figures of unresolved peaks having large FWHMs. The patterns of the reciprocal lattice for each orientation are not well resolved, which then impacts the refinement of an introduced texture models (parameters for spherical texture and/or fiber texture).

MULTEX 3 and all other commercial software apply a texture component method. The basic idea of the texture component method is the approximation of X-ray textures in the form of the orientation distribution function (ODF) using a set of simple distribution functions or texture components, as published by Helming (1996). Hereby two types of model functions, fiber components and spherical components are used to describe the orientation density (texture) of the sample. The spherical components are fully described by three parameters: the preferred orientation, the scatter width and the intensity or volume fraction. This implies that for each volume element of particular texture a spherical texture component has to be introduced to the overall texture model.

The fiber components are also described by three measures: the fiber axes along the crystallites are tilted, the scatter width and the intensity or volume fraction. In addition to spherical texture components and fiber texture components also a random texture component can be introduced to the modeling. The computational iterations for optimizing the given model and to improve the goodness of fit (e.g. as $\chi^2 = \Sigma(I_{observed} - I_{calculated})^2/I_{calculated}$) do not converge and the individual results become arbitrary.

Texture Analysis on a Molybdenum Single Crystal in (001) and (011) Orientation

The data file for this example was provided by Bruker. Analysis of the data was performed at INL using Bruker Multex 3 software. The texture of this single crystal is complete since only one orientation of this crystallite is present. The texture of single crystal molybdenum is modeled in Figure 3. The experimental intensities of the pole figures describe the actual counts of the diffracted intensities as recorded by the instrument. The recalculated (modeled) intensities describe the fitted intensities after applying a texture model with elements of spherical and/or fiber texture using Multex 3 software.

The difference intensity plot displays the difference between observed (experimental) intensities and modeled (recalculated) intensities as $I_{dif} = I_{observed} - I_{calculated}$. The colors from measurement (experimental) and modeling (recalculated) represent the intensity range. Green indicates the section of the reciprocal space examined and a low background of about 0, while white indicates no information from the measurement within this reciprocal crystal space. If the sample shows distinct texture, pole figures appear in red as 2-dimensional narrow peaks indicating preferred orientation. The black squares show the computational pole figures as a function of crystal orientation. In the texture modeling used to analyze this data, parameters for spherical texture and fiber texture were introduced and, as a result of numerical iterations, the χ^2 value was minimized ($\chi^2 = \Sigma(I_{observed} - I_{calculated})^2/I_{calculated}$). The χ^2 value represents the goodness of fit and approaches lower values after the modeled intensities are approximately matching the experimental intensities. This is displayed as difference intensities, which are grey for a small mismatch and blue for larger mismatches.

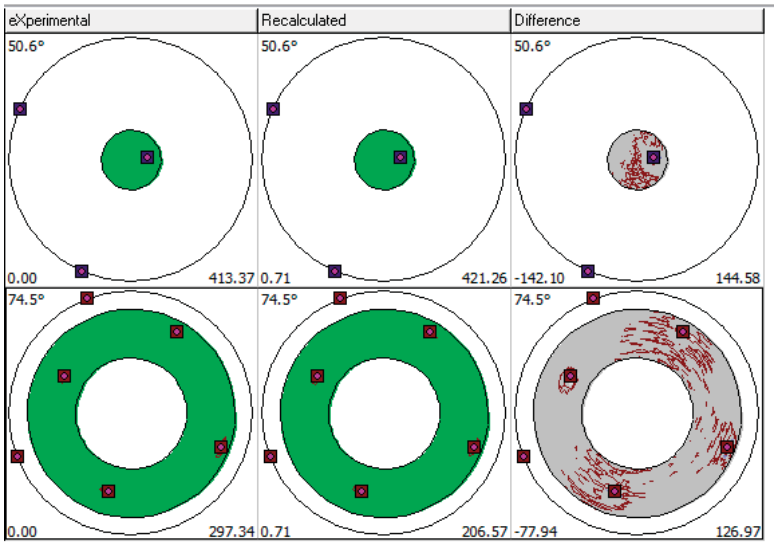

Figure 3. Measured and calculated pole figure of single crystal Mo sample.
Top: (001) Bottom: (011)

The calculated pole figures without the experimental or difference for each direction are displayed in Figure 4.

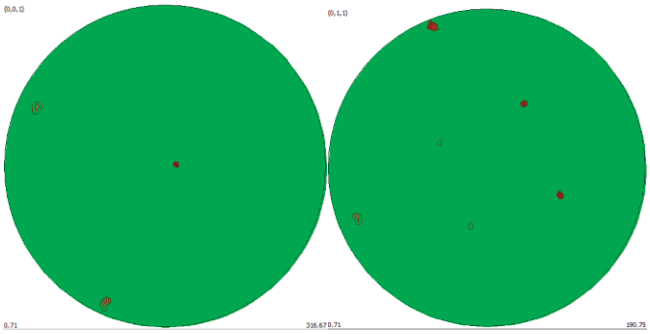

Figure 4. Calculated pole figure of a single crystal molybdenum in (001) (left) and in (011) (right) without the calculated pole figure displayed. The calculated/modeled MRD (multiple intensity of random distribution) values range from 0.7 to about 317.

The large number of 317 indicates virtually complete texture in this example, since it was measured on an aligned single crystal for reasons of demonstration. In the assigned orientations (001) & (011), the pole figures indicate an over-representation of diffracted intensities compared with random non-textured conditions of 317 times for the (001) direction and and 191 times for the (011) direction. This over-representation indicates the significance of texture in (001) and (011) since the single crystal is aligned in either direction. For the polycrystalline case, all crystallites would be oriented in either direction.

The inverse pole figures provide texture information in the normal direction (ND), the transverse direction (TD), and the rolling direction (RD) and are displayed in Figure 5. **NOTE**: *RD, TD and ND are labels used by the texture measurement software to represent orthogonal axes applied to the sample and do not necessarily imply the sample has been rolled, as it has not in this case. There was no directionality in the fuel pin samples.*

In the display of inverse pole figures using Multex 3, the green color represents virtually no intensity above background, and an iso-line of 0 denotes random conditions relative to the orientation. With increasing deviation from random, the color shifts towards red. More important than the colors help to

observe the nature of the contour lines indicating the orientation of the poles relative to the crystallographic orientation. At highest intensity the iso-lines in the pole figure of modeled copper indicates a 6-fold over-representation of this orientation compared with the non-textures case.

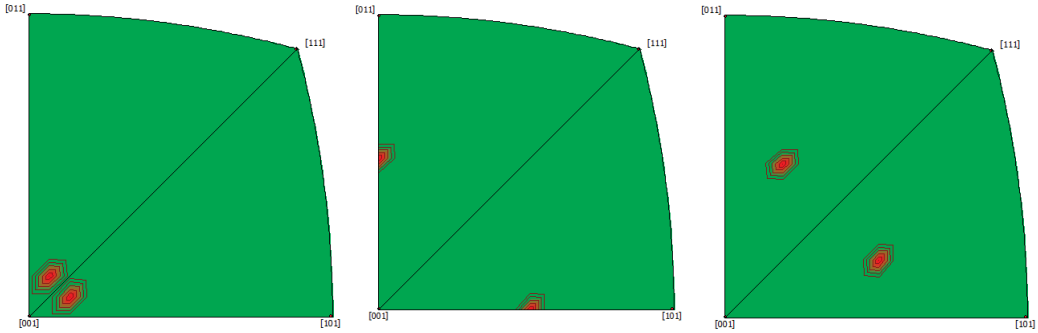

Figure 5. Inverse pole figures of single crystal molybdenum.
Left: texture in ND with MRD ranging from 0.7 to 29. Center: texture in TD with MRD from 0.7 to 69. Right: texture in RD with MRD from 0.7 to 38.

Texture Analysis of Rolled Copper foil in (111) Orientation

The XRD data for this example was obtained from a copper attenuator (highly textured copper foil after cold rolling) using the Bruker D8 Discover at INL and the analysis of the data was performed using Bruker Multex 3 software. This sample represents a material with strong texture, though not at the limiting condition of the single crystal as in the molybdenum example.

For modeling the texture of this cold-rolled copper plate in (111) the Laue symmetry (*m-3m*) and the published lattice parameter were used. The pole figure could be reproduced after the introduction of an orthorhombic sample "symmetry" which adds more parameters to the pole figure modeling, representing the generation process of the texture in the material. Unlike the crystal symmetry (*F4/m-32/m*), the sample symmetry produces different orientations of the crystal lattice relative to the sample and can be considered as "fuzzy symmetry".

To model the texture we further introduced spherical texture components and fiber texture components. The Multex software optimizes these parameters by iterations to minimize the χ^2 value. This goodness of fit is defined as $\chi^2 = \Sigma(I_{observed} - I_{calculated})^2/I_{calculated}$). If distinct texture is present, the computational iterations converge to a concrete result in order to quantify texture, e.g. after applying a cold working process step. Modeling of the texture of Cu (111) was successful and the calculated/modeled pole figure matches well with the measurement as seen in Figure 6.

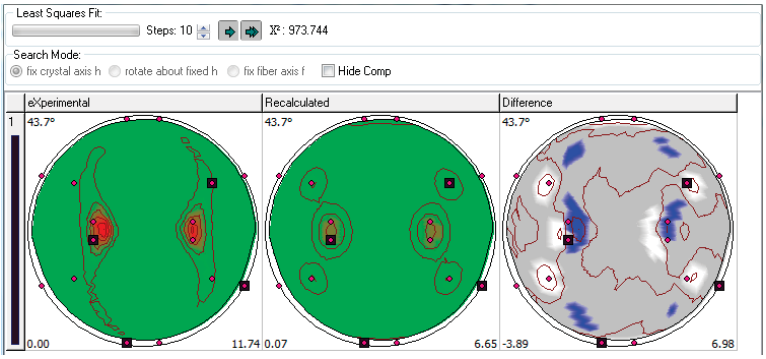

Figure 6. Measured and calculated pole figure of a copper foil.

The pole figure of copper was modeled based on an orthorhombic sample symmetry which was induced from the rolling process and on the cubic symmetry of the crystal structure. The calculated pole figure is shown in Figure 7.

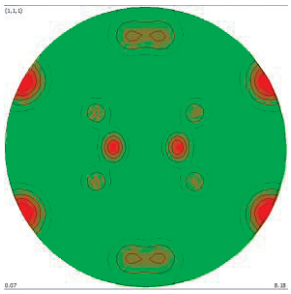

Figure 7. Calculated pole figure of a copper foil in (111) based on an orthorhombic sample symmetry (imposed by cold rolling) and the cubic crystal structure in Laue class *m-3m*.

The texture in the copper foil was introduced through cold-working which induces strain-hardening and residual stress, but also elongates the crystallites in the rolling direction to provide the pole figure as measured. Texture, especially in metals and alloys, is a representation of the dominant grain orientations within the metal microstructure rather than a representation of its crystal structure.

Even though copper is cubic (space group *F4/m-32/m*), its physical properties, like hardness and thermal conductivity, are not isotropic, but anisotropic tensor properties. On the other hand, loose powders of cubic crystallites of e.g. halite (NaCl) will not exhibit much preferred orientation spreading them out, e.g. on a XRD sample holder, compared with hexagonal crystallites such as graphite, which will be predominantly oriented in (001) and will show significant fiber texture as monolithic compacts. The MRD values for the rolled copper range from 0 to about 8 indicating strong texture. This is also apparent by observing the contour regions of both the measured and calculated pole figures. Notice that these regions are very distinct and spaced symmetrically. The pole figure is showing diffraction peaks profiles characterized by small FWHMs.

The inverse pole figures provide texture information in the normal direction (ND), the transverse direction (TD), and the rolling direction (RD) and are shown in Figure 8.

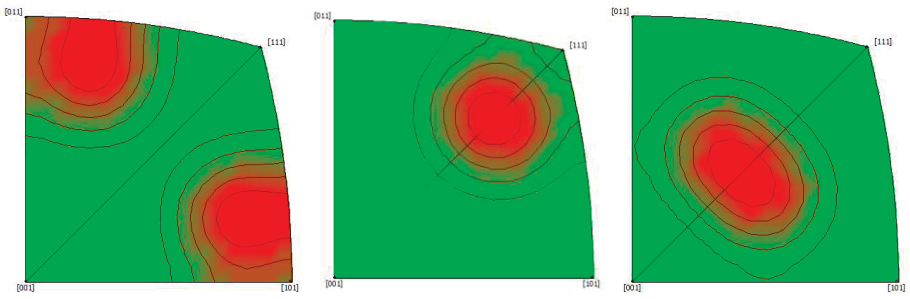

Figure 8. Inverse pole figures of rolled copper foil.
Left: texture in ND. Center: texture in TD. Right: texture in RD.

Texture Analysis of Alumina (Al_2O_3) Powder: Random Orientation Standard

This sample was prepared by pressing the NIST certified standard corundum powder into pellet form. It was prepared at INL to provide an example of texture mapping for a virtually completely random orientation. This sample provides the limiting condition on the other end of the texture spectrum from the single crystal molybdenum. Data was gathered on the Bruker D8 Discover XRD at INL and analysis of the data was performed using Bruker Multex 3 software. Figure 9 shows the measured, calculated and difference pole figures of the sample.

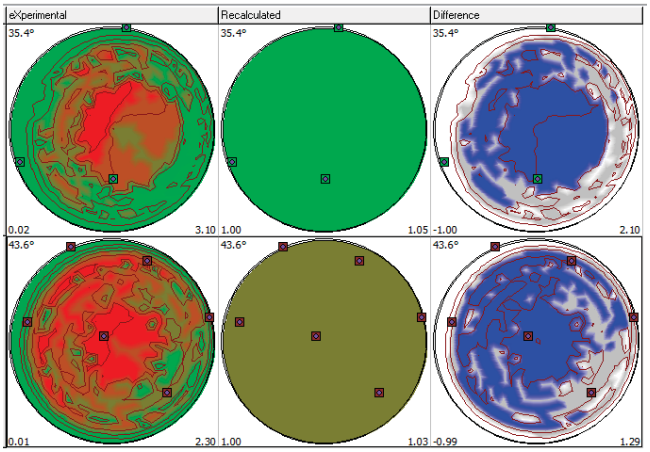

Figure 9. Measured and calculated pole figures of virtually random corundum powder in the (104) orientation (top), and the (113) orientation (bottom).

This example shows that, because having a random texture in the alumina powder example, texture modeling does not provide stable results since the iterations of the texture model do not converge to texture parameters of concrete values. As a result, modeling produces recalculated pole figures of random orientation which is indicated by the constant intensities in the modeled pole figures and indicated by rather constant iso-lines between 1 and 1.05 for (104) or 1 to 1.03 for the (113) orientation.

These samples have virtually no texture and it was confirmed by texture modeling. The MRD values for this sample range from 0.02 to 3.10 for (104) orientation, which is a significantly lower range than MRD values for the highly textured samples shown previously. The calculated pole figures for each orientation are displayed in Figure 10. Texture modeling of data with virtually random orientation does not produce a particular result since the iterations of the refinement do not converge.

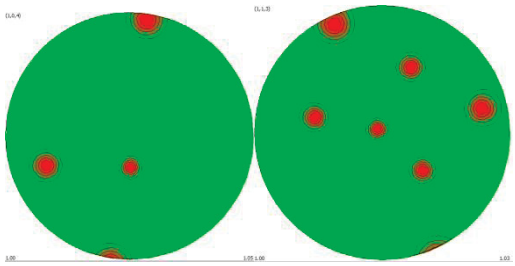

Figure 10. Calculated pole figures of corundum powder.
Left: pole figure in (104) with MRD ranging from 1 to 1.05. Right: pole figure in (113) with MRD from 1 to 1.03.

The resulting inverse pole figures provide texture information in the normal direction (ND), the transverse direction (TD), and the rolling direction (RD) and are displayed in Figure 11.

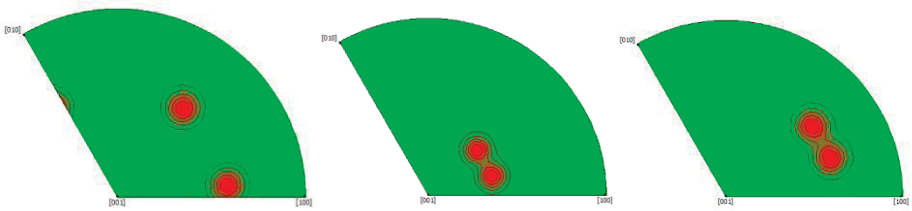

Figure 11. Inverse pole figures of corundum powder.
Left: texture in the ND with MRD ranging from 1 to 1.03. Center: texture in the TD with MRD from 1 to 1.03. Right: texture in the RD with MRD from 1 to 1.03.

Texture Analysis of Uranium

A pure uranium fuel sample (non heat treated) was analyzed for the sake of comparison. This material was legacy feedstock which appears to have been rolled or swaged, but it is not certain how it was actually deformed. Data from the sample was acquired using the Bruker D8 Discover.

A bulk run was performed followed by pole figure runs in the (110), (021), (111), and (112) directions. Bulk XRD data of α-uranium (1126) was analyzed using a combination of Rietveld structure refinement and peak profile fitting. For all phases other than α-uranium Rietveld refinement was applied, while α-uranium was fitted using Pawley type peak profile fitting which does not require a structure model and allows for an unconstrained fitting for the (110) and (021) diffraction peak of α-uranium. The ratio of the relative peak intensities of $I_{(110)}/I_{(021)}$ was found to be 0.951 and the absolute peak intensity ratio was found to be 0.907. A ratio of 0.738(2) for relative intensities and a $I_{(110)}/I_{(021)}$ ratio of 0.702(1) for absolute peak intensities is considered random using this experimental set-up.

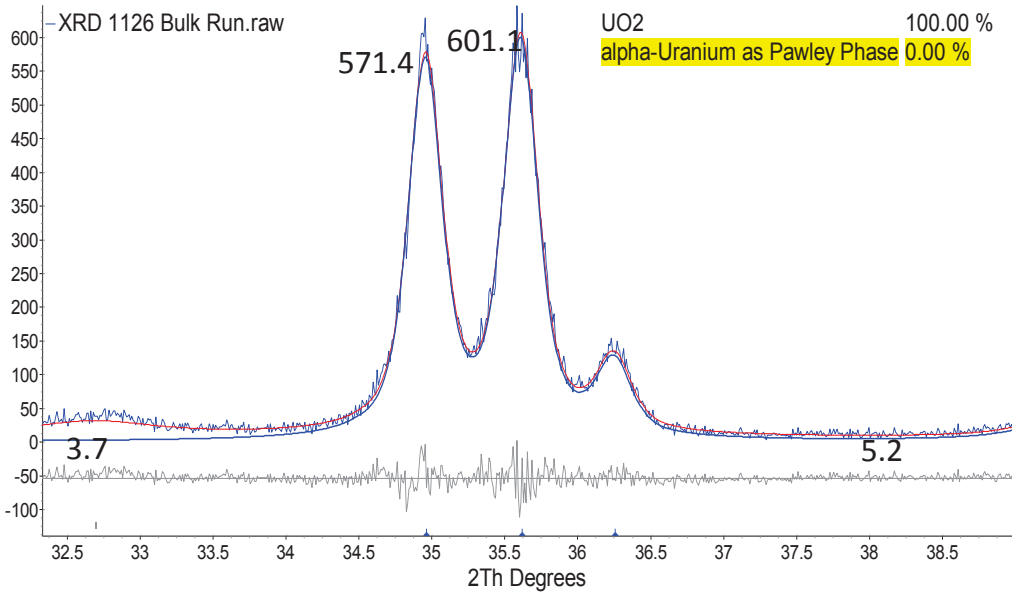

Figure 12. Pawley fit for α-uranium to determine the relative peak intensity ratio in α-Uranium (sample 1126). The specimen also contains about 22 wt.-% UO_2 as a result of surface oxidation. Using this optimized method, a relative peak intensity ratio $I_{(110)}/I_{(021)}$ of 0.951 was determined

Pole figure data was analyzed using Bruker Multex 3 software. Modeling the texture of α-uranium was somewhat successful using a combination of spherical and fiber texture. This means that for texture modeling, besides Laue symmetry and sample symmetry ("fuzzy symmetry" of texture generation), we are introducing parameters to model spherical texture and fiber texture. Using spherical texture

parameters allows for adjusting crystallite orientation based on the pole figures of the reciprocal lattice in the 3-dimensional crystal space. Fiber texture is modeled by fixing on specific orientation (e.g. (0001) in monolithic graphite) and adjusting of the rotation of the crystallites along (0001). Texture modeling using Multex allows the refinement of multiple sets of spherical and fiber texture parameters.

The measured and calculated pole figures are shown in Figure 13.

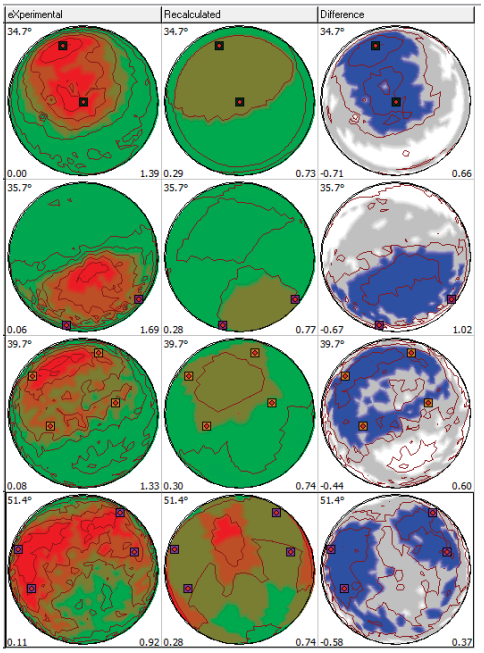

Figure 13. Measured and calculated pole figure of α-uranium in (110), (021), (111), and (112) from top to bottom.

The calculated pole figure of α-uranium shows weak texture. The iso-lines range between 0.3 and 0.8 and poles (2 dimensional peaks) have large FWHMs. For each orientation (110), (021), (111), and (112) increased diffracted intensities in the modeled pole figures are indicated as red areas. The inverse pole figures show that in ND (normal direction ≈ X-ray beam direction) the intensities in (-100) and (100) (along lattice parameter ***a***) are increased. The pole figure of α-uranium was modeled based on triclinic sample symmetry assuming no major impact by processing, using the *mmm* Laue class (space group *Cmcm*) and the published lattice parameter of this phase (Figure 14).

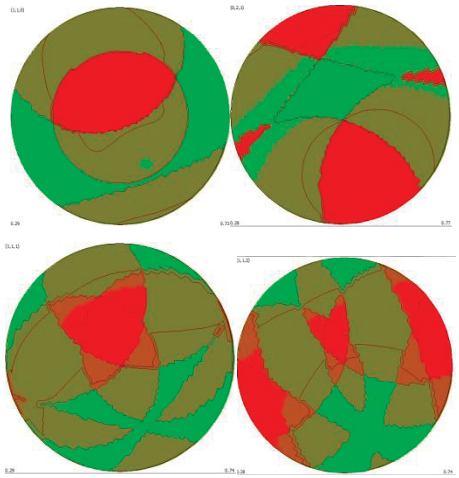

Figure 14. Calculated pole figure of α-uranium in (110) (left top), and (021) (right top), as well as in (111) (bottom left) and in (112) (bottom right).
The MRD is in the range between 0.3 and 0.8.

The inverse pole figures provide texture information in the normal direction (ND), the transverse direction (TD), and the rolling direction (RD), and are displayed in Figure 15.

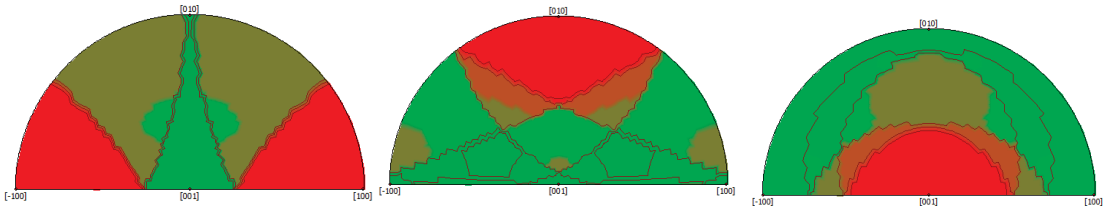

Figure 15. Inverse pole figures of α-uranium.
Left: calculated texture in ND. Center: calculated texture in the TD. Right: calculated texture in RD. The MRD ranges from 0.3 to 0.8. Since the chosen (hkls) are not independent, standard inverse pole figures cannot be displayed

EBRII and FFTF Samples

These U-10wt%Zr samples were taken from as-built archive U-10Zr pins built for EBR-II and FFTF experiments. The EBR-II pin had a single 13.5" fuel slug, while the FFTF pin had two 18" slugs stacked together to form the fuel column. They had been injection cast (rapidly cooled), and inserted into stainless steel cladding with sodium bond.

The sample locations (axially) are listed in Tables 2 and 3. Since there were two stacked slugs in the FFTF fuel column, the '1' and '2' immediately following the 'R' indicates which of the two slugs the sample contains. 'R' refers to a section taken near axial location a, b, or c. Since the fuel slug could be placed in the cladding with either end of the casting up, that orientation detail was lost. Figure 16 shows a sketch of a typical mount configuration. The transverse section samples were removed from the metallography mount and used by themselves for this study. No additional sample preparation other than removal from the mount was necessary. The longitudinal sections were not used for texture measurements.

Table 2. Sample locations for fuel and cladding from EBR-II fuel element.

Region of Interest	Location from the Spade End of Element
Ra (Fuel)	1/4 in. to 1 in.
Rb (Fuel)	6-3/8 in. to 7-1/8 in.
Rc (Fuel)	12-1/2 in. to 13-1/4 in.

Table 3. Sample locations for fuel and cladding from FFTF fuel element.

Region of Interest	Location from the Spade End of Element
R1a (5% of Fuel Length)	1 ½" to 2 ¼"
R1c (40% of Fuel Length)	14" to 14 ¾"
R2a (60% of Fuel Length)	21 ¼" to 22"
R2c (95% of Fuel Length)	33 7/8" to 34 5/8"

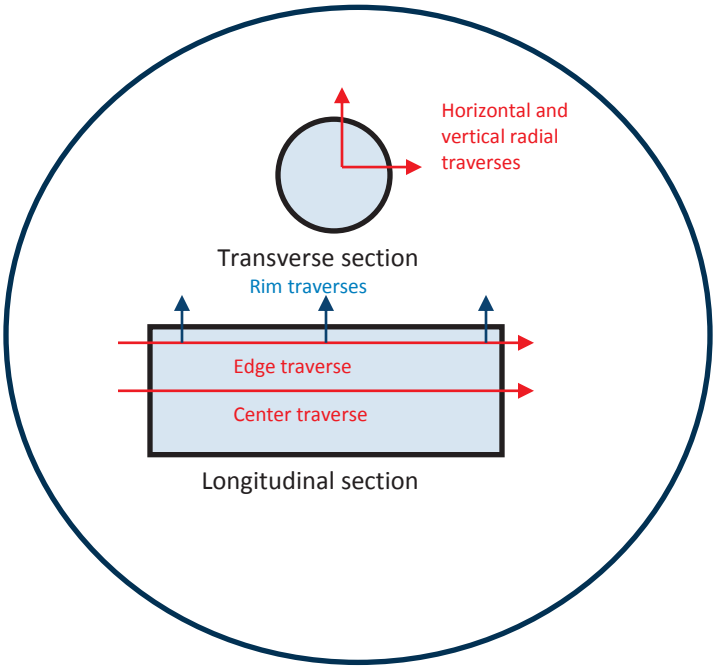

Figure 16. Schematic showing geometry of samples mounted into the metallography mount.

The numbering system seems quite complicated but the important are the first two letters in the case of an EBR-II pin sample and the first three characters in the cast of an FFTF pin sample.

Those used for this texture study include:

1. R1a2R1a5a (U10Zr)
2. R1c2R1c5a (U10Zr)
3. R2c2R2c5a (U10Zr)
4. R2a2R2a5a (U10Zr)
5. Ra2Ra5a (U10Zr)

The pins had been bonded, meaning heated to ~500°C for an hour (to allow the Na to wet the stainless steel internal surface) while being impacted (raised and dropped slightly) in the case of EBR-II pins, or heated to ~500°C for an hour while being vibrated in the case of FFTF pins. They were not expected to have a strong texture, if any. For EBR-II pins ('R' w/o a number, like number 5), the Ra2 refers to the number 2 transverse cross-section at 'a', the one mounted for metallography.

The FFTF slug samples just have one more complication, whether it was the first, or '1', slug (sitting on the lower end plug) or the second, '2', slug above the '1'. The number '1' or '2' immediately following the 'R' tells which slug the sample came from. The lower case letter following this refers to the axial location, 'a' or 'c'. The last four (EBR-II) or five (FFTF) characters refer to the companion longitudinal sample which was not analyzed for texture.

Texture Analysis of R1a2R1a5a (U10Zr)

Data for R1a2R1a5a (U10Zr) was obtained using the Bruker D8 Discover XRD at INL and data analysis was performed at INL using Bruker Multex 3 software. The texture of the α-uranium phase of R1a2R1a5a was analyzed on patterns taken in the (110), (111), and (112) orientation based on the combination of a spherical and a fiber texture model with crystal symmetry in the Laue class *mmm*. These particular directions were chosen because they are the strongest peaks from the α-uranium phase that have no overlap from the δ-UZr_2 phase. Modeling the texture of α-uranium was only somewhat successful due to the lack of texture and the large FWHM of the diffracted intensities. Thus, the refinements did not converge to a particular result (lack of convergence suggests very weak or no texture). The measured and calculated pole figures are shown in Figure 17.

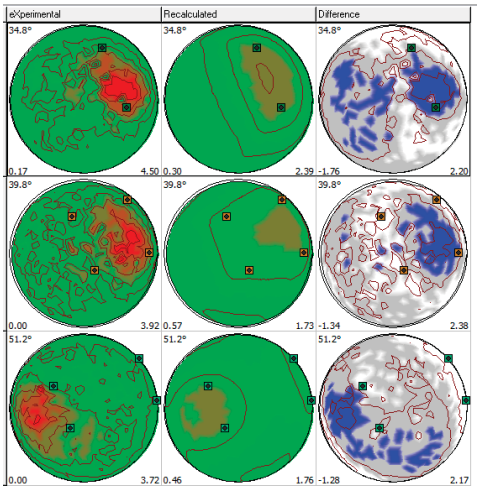

Figure 17. Measured and calculated pole figures of the α-uranium phase of R1a2R1a5a (U10Zr) in (110) (top), (111) (center) and in (112) orientation (bottom).

The calculated pole figures for each orientation are displayed in Figure 18.

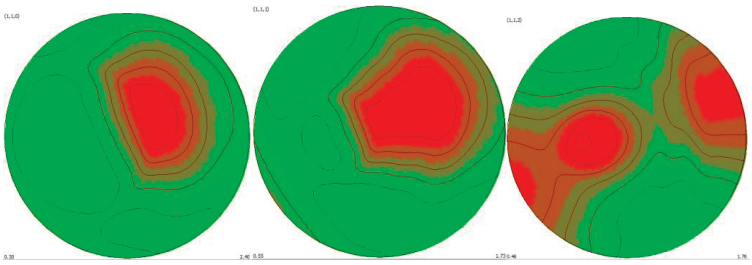

Figure 18. Calculated pole figures of the α-uranium phase of R1a2R1a5a (U10Zr).
Left: pole figure in (110) with MRD ranging from 0 to 2.4. Center: pole figure in (111) with MRD from 0.5 to 1.7. Right: pole figure in (112) with MRD from 0.5 to 1.8.

The inverse pole figures provide texture information in the normal direction (ND), the transverse direction (TD), and the rolling direction (RD), and are displayed in Figure 19.

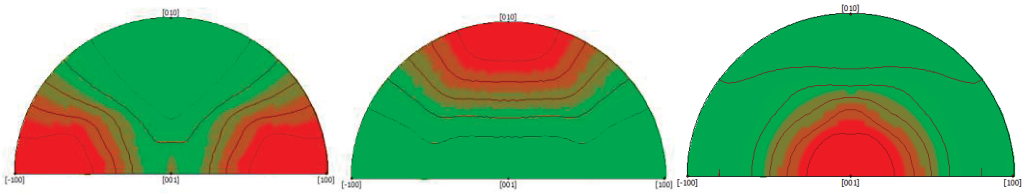

Figure 19. Inverse pole figures of the α-uranium phase of R1a2R1a5a (U10Zr).
Left: calculated texture in ND with MRD ranging from 0.3 to 2. Center: calculated texture in TD with MRD from 0.4 to 2.6. Right: calculated texture in RD with MRD from 0.5 to 1.8.

Texture Analysis of R1c2R1c5a (U10Zr)

Data for R1c2R1c5a (U10Zr) was obtained using the Bruker D8 Discover XRD at INL and data analysis was performed using Bruker Multex 3 software. The texture of the α-uranium phase of R1c2R1c5a was analyzed on patterns taken in the (110), (111), and (112) orientations. Modeling the texture of α-uranium was only somewhat successful due to the lack of significant texture and the large FWHM of the diffracted intensities. Thus, the refinements did not converge to a particular result. The lack of convergence is most likely an indication of random orientation or only insignificant texture. Figure 20 shows the measured and calculated pole figures.

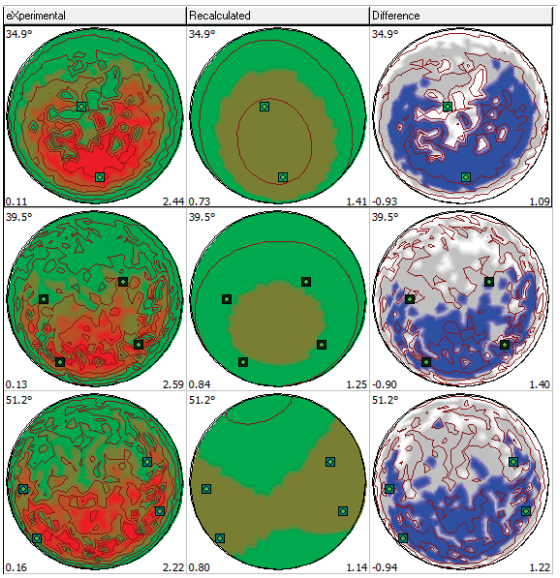

Figure 20. Measured and calculated pole figures of the α-uranium phase of R1c2R1c5a (U10Zr) in (110) (top), (111) (center) and in (112) orientation (bottom).

The calculated pole figures for each orientation are displayed in Figure 21.

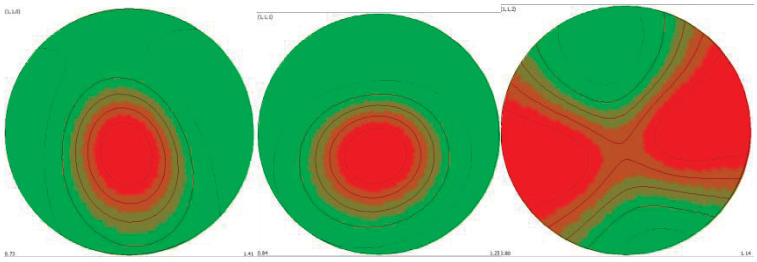

Figure 21. Calculated pole figures of the α-uranium phase of R1c2R1c5a (U10Zr).
Left: pole figure in (110) with MRD ranging from 0.7 to 1.4. Center: pole figure in (111) with MRD from 0.8 to 1.3. Right: pole figure in (112) with MRD from 0.8 to 1.1.

The inverse pole figures provide texture information in normal direction (ND), transverse direction (TD), and rolling direction (RD), and are displayed in Figure 22.

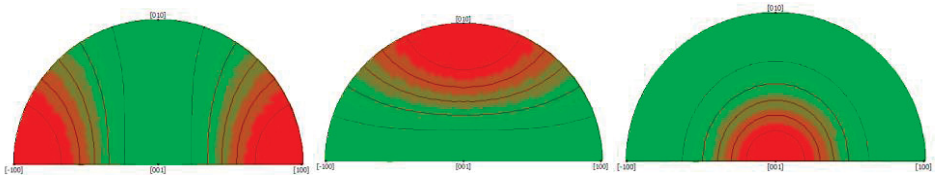

Figure 22. Inverse pole figures of the α-uranium phase of R1c2R1c5a (U10Zr).
Left: calculated texture in ND. Center: calculated texture in TD, and right: calculated texture in RD. The MRD ranges from 0.7 to 1.5. Since the chosen (hkls) are not independent, standard inverse pole figures cannot be displayed.

Texture Analysis of R2c2R2c5a (U10Zr)

XRD-texture data for R2c2R2c5a (U10Zr) was obtained using the Bruker D8 Discover at INL and the subsequent data analysis was performed using Bruker Multex 3 software. The texture of the α-uranium phase of R2c2R2c5a was analyzed based on diffraction patterns taken in the (110), (111), and (112) orientations. Modeling the texture of the α-uranium phase was only somewhat successful due to the lack of texture and the large FWHM of the diffracted and modeled intensities within the pole figures. Thus, the refinements did not converge to a particular result which indicates the lack of texture or very minor texture within the microstructures. This is also indicated by the low MRD values which determine the texture-related relative intensity changes in multiples of random distribution. Hereby the measured intensities are ranging between 0 and 3 MRD and the modelled intensities between 0.5 and 1.7 indicating the presence of insignificant texture (Figure 22).

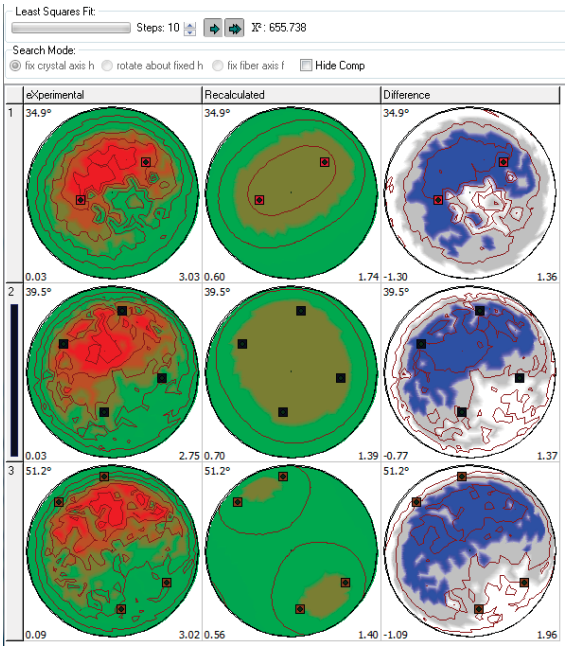

Figure 23. Measured and calculated pole figures of the α-uranium phase of R2c2R2c5a (U10Zr) in (110) (top), (111) (center) and in (112) orientation (bottom).

The calculated pole figures for each orientation are displayed in Figure 24.

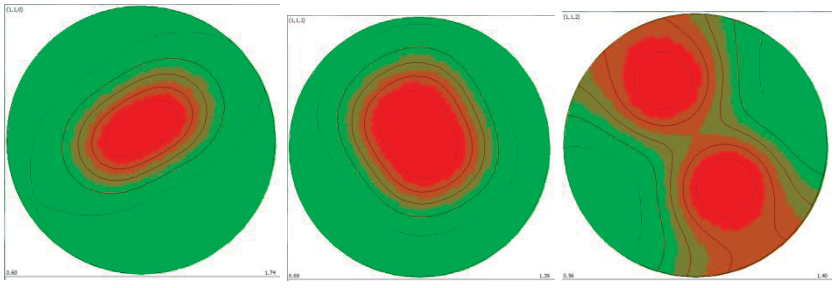

Figure 24. Calculated pole figures of the α-uranium phase of R2c2R2c5a (U10Zr).
Left: pole figure in (110) with MRD ranging from 0.6 to 1.7. Center: pole figure in (111) with MRD from 0.7 to 1.4. Right: pole figure in (112) with MRD from 0.6 to 1.4.

The inverse pole figures provide texture information in normal direction (ND), transverse direction (TD), and rolling direction (RD), and are displayed in Figure 25.

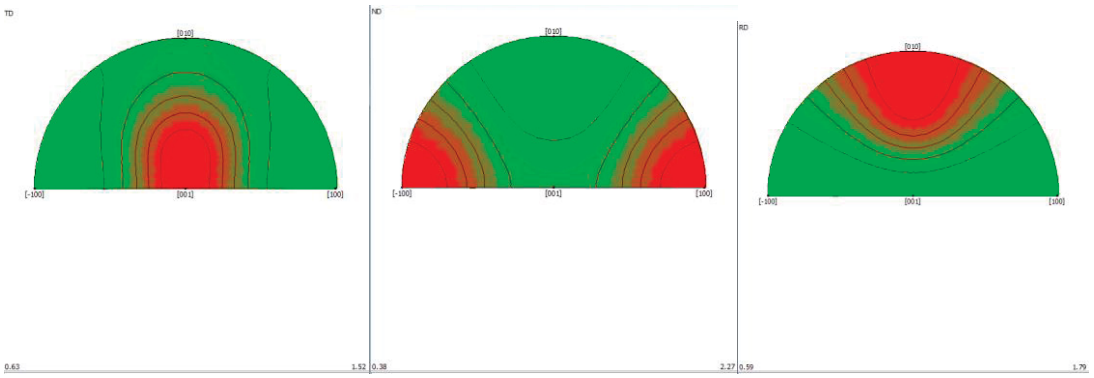

Figure 25. Calculated inverse pole figures for R2c2R2c5a (U10Zr) in normal direction (ND, top left), transverse direction (TD, top right) and rolling direction (RD, bottom).
The MRD values are indicated, and are ranging from 0.3 to 2.3.

Texture Analysis of R2a2R2a5a (U10Zr)

XRD-texture data for R2a2R2a5a (U10Zr) was obtained using the Bruker D8 Discover X-ray diffractometer at INL and the subsequent data analysis was performed using Bruker Multex 3 software. The texture of the α-uranium phase of R2a2R2a5a was analyzed based on diffraction patterns taken in the (110), (111) and (112) orientations. Modeling the texture of α-uranium was only somewhat successful due to the lack of texture and the large FWHM of the diffracted and modeled intensities within the pole figures. Thus, the refinements did not converge to a particular result which indicates the lack of texture or very minor texture within the microstructures. This is also indicated by the low MRD values which determine the texture-related relative intensity changes in multiples of random distribution. The measured intensities are range from 0 to 3 and the calculated intensities range from 0.5 to 2 indicating the presence of insignificant texture (Figure 26).

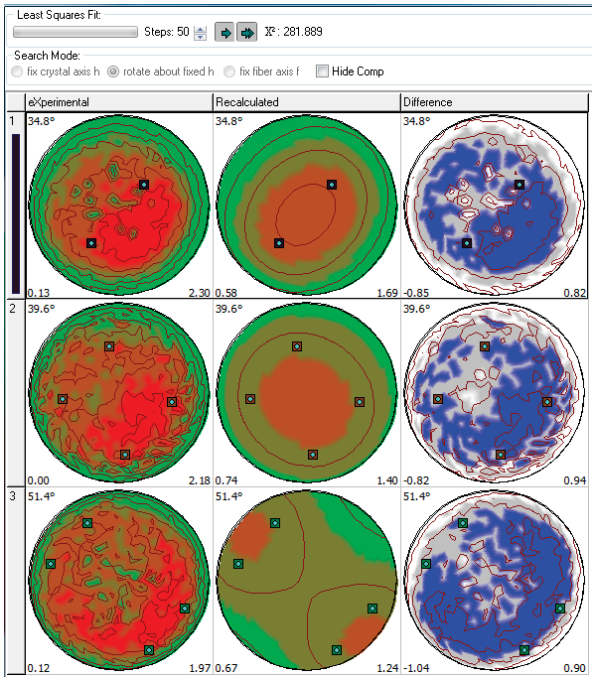

Figure 26. Measured and calculated pole figures of the α-uranium phase of R2a2R2a5a (U10Zr) Radial in (110) (top), (111) (center) and in (112) orientation (bottom).

The calculated pole figures for each orientation are displayed in Figure 27.

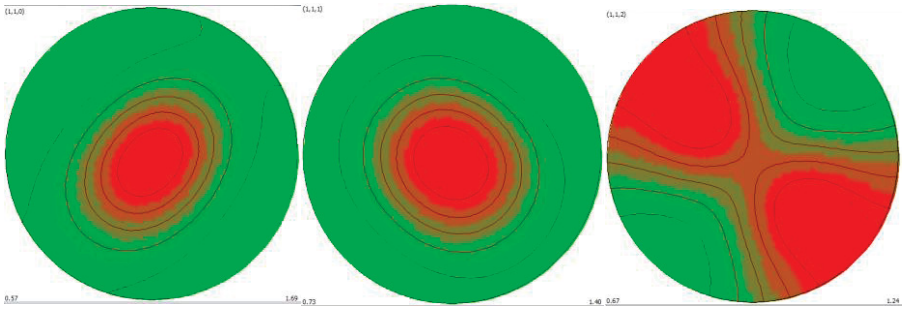

Figure 27. Calculated pole figures of the α-uranium phase of R2a2R2a5a (U10Zr).
Left: pole figure in (110) with MRD ranging from 0.6 to 1.7. Center: pole figure in (111) with MRD from 0.7 to 1.4. Right: pole figure in (112) with MRD from 0.7 to 1.2.

The inverse pole figures provide texture information in normal direction (ND), transverse direction (TD), and rolling direction (RD), and are displayed in Figure 28.

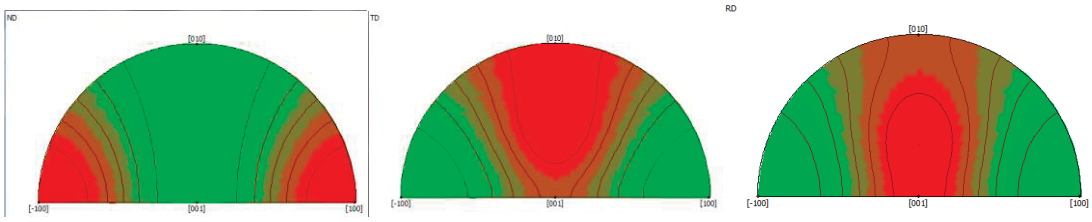

Figure 28. Calculated inverse pole figures for R2a2R2a5a (U10Zr) in normal direction (ND, top left), transverse direction (TD, top right) and rolling direction (RD, bottom).
The MRD values are indicated, ranging from 0.6 to 2.0.

Texture Analysis of Ra2Ra5a (U10Zr)

XRD-texture data for Ra2Ra5a (U10Zr) was obtained using the Bruker D8 Discover X-ray diffractometer at INL and the subsequent data analysis was performed using Bruker Multex 3 software. The texture of the α-uranium phase of Ra2Ra5a was analyzed based on diffraction patterns taken in the (110), (111), and (112) orientations. The sample does not show texture significant enough to allow for quantitative modeling. The FWHMs of the calculated pole figures were large and the refinements did not converge to a particular result which indicates the lack of texture or very minor texture within the microstructures. This is also indicated by the low MRD values which determine the texture-related relative intensity changes in multiples of random distribution. The measured intensities are ranging between 0 and 2.5 MRD and the calculated intensities range between 0.8 and 1.3 2, indicating that there was no measurable texture present (Figure 29).

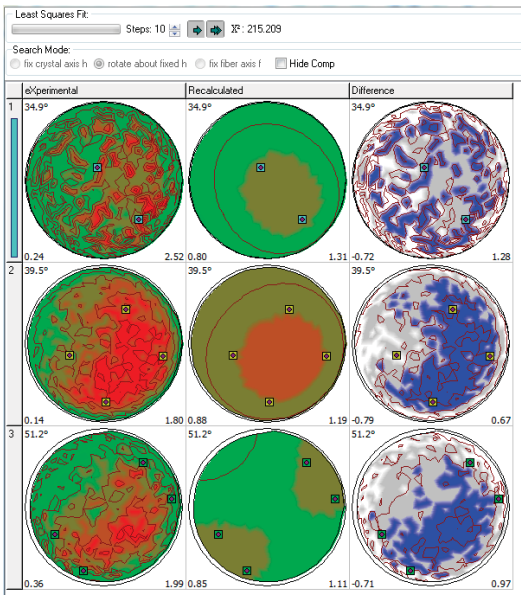

Figure 29. Measured and calculated pole figures of the α-uranium phase of Ra2Ra5a (U10Zr) Radial in (110) (top), (111) (center) and in (112) orientation (bottom).

The calculated pole figures for each orientation are displayed in Figure 30.

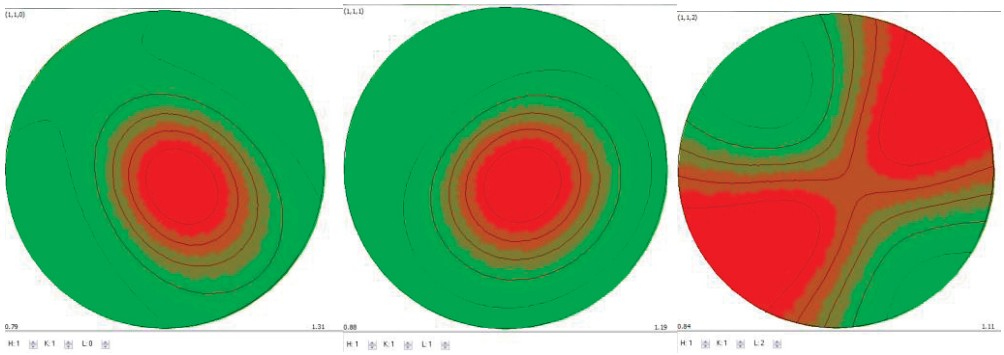

Figure 30. Calculated pole figures of the α-uranium phase of Ra2Ra5a (U10Zr).
Left: pole figure in (110) with MRD ranging from 0.8 to 1.3. Center: pole figure in (111) with MRD from 0.9 to 1.2. Right: pole figure in (112) with MRD from 0.9 to 1.1.

The inverse pole figures provide texture information in normal direction (ND), transverse direction (TD), and rolling direction (RD) and are displayed in Figure 31.

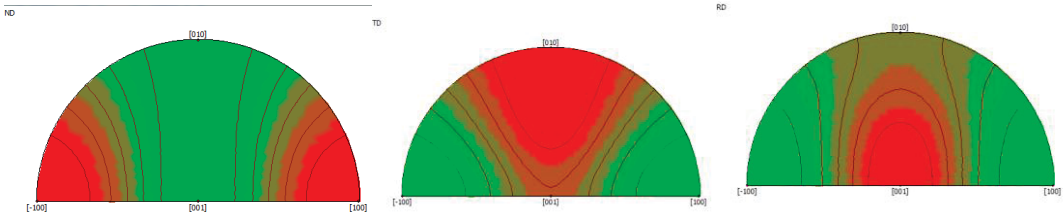

Figure 31. Calculated inverse pole figures for Ra2Ra5a (U10Zr) in normal direction (ND, top left), transverse direction (TD, top right) and rolling direction (RD, bottom).

U5Fs (for 5Fs = 2.44Mo-1.95Ru-0.3Rh-0.2Pd-0.09Zr-0.02Nb)

A U5Fs rod was obtained from legacy material in the Analytical Laboratory and a small section of this rod was cut to prepare an XRD sample. No additional sample preparation was performed. Data was collected on the Bruker D8 Discover XRD and Rietveld refinement was performed using Topas 4.2. The intent of this work was to perform bulk XRD analysis followed by pole figure generation and to further compare the traditional peak ratio method (Sturcken & Walter) with the method of quantitative XRD-based texture analysis. However, phase analysis of this sample determined γ-uranium rather than α-uranium as major phase and could not be used for this purpose without further treatment. Figure 32 shows the results of the Rietveld analysis of this sample.

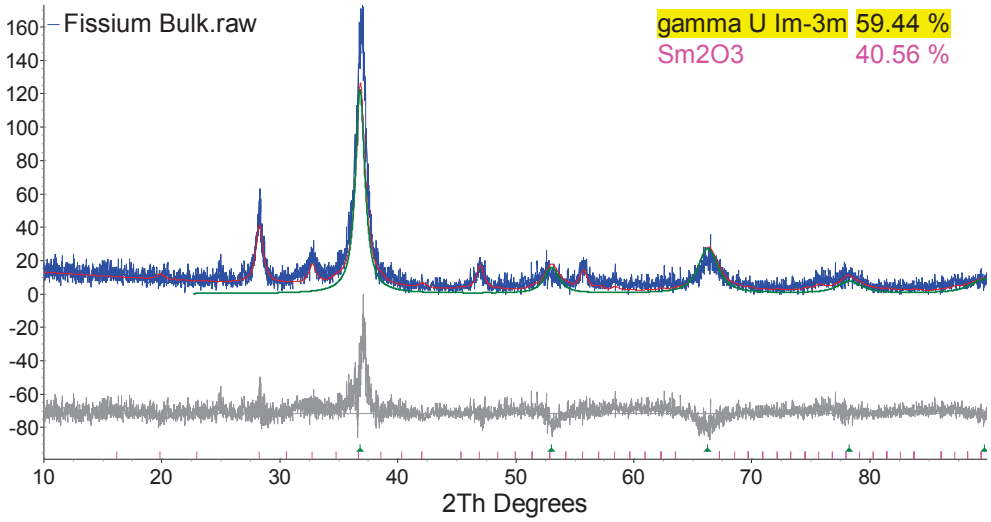

Figure 32. Pattern and Rietveld analysis of U5Fs before heat treatment.
The pattern was fitted based on the crystal structures of a γ-uranium solid solution phase, and a Sm_2O_3-based solid solution phase.

The pattern shows low counts and a γ-uranium-based solid solution phase was identified as major phase. The remaining diffracted intensities were fitted based on a Sm_2O_3 solid solution phase. The lattice parameter were refined to $\boldsymbol{a}$ = 3.453(1) Å for uranium, which is slightly smaller than pure γ-uranium and to $\boldsymbol{a}$ = 10.946(5) Å for the cubic lanthanide phase which is slightly larger than pure Sm_2O_3.

While this result was somewhat unexpected, it can be explained by the history of this U5Fs rod. The lack of thermal treatment may have prevented the γ-uranium phase to reach equilibrium as α-uranium (Sturcken & Walter, J. Nuclear Materials. 50, 1974, 69-82). Therefore, the U5Fs sample was heat treated (heated to 500°C and held for 2 hours) to achieve equilibrium conditions and to convert the γ-uranium phase to α-uranium. Figure 33 shows the results of the Rietveld refinement of the post annealed sample. The major phase in this sample is α-uranium (59 wt.-%) with contributions from γ-uranium (12 wt.-%) and uranium dioxide (28 wt.-%). In addition, three unidentified peaks with weak intensities at d_{hkl} = 7.18 Å, 3.58 Å, and 2.86 Å were observed. Additional knowledge about the history of this particular sample could have helped to identify the remaining minor phase(s). However, based on the bulk data ofU5Fs after annealing, we collected pole figures in the orientations (110), (111), and (112) to engage in texture analysis of the α-uranium phase. In doing so, we expected a minor interference of the pole figures (110) and (111) with the (011) diffraction peak of γ-uranium.

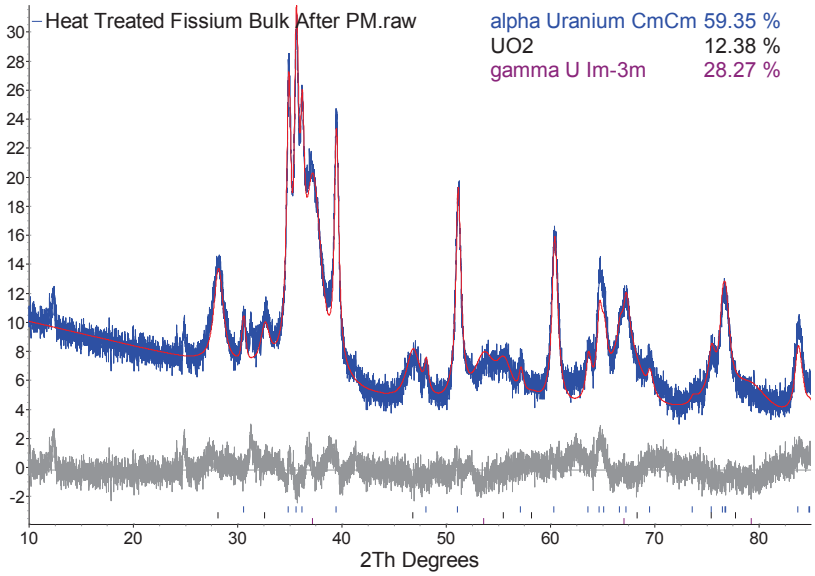

Figure 33. XRD pattern and Rietveld structure refinement of U5Fs sample after heat treatment.

Texture data from the U5Fs material was collected for the α-uranium diffraction peaks (110), (111), and (112) using the Bruker D8 Discover at INL in order to compare the data from this sample to data from the U10Zr samples. Subsequent data analysis and modeling were performed using Bruker Multex 3 software. The α-uranium phase of U5Fs does not show texture sufficient to allow for quantitative modeling. The modeling iterations did not converge and the FWHMs of the calculated pole figures are large, which indicates the lack of measurable texture or the presence of very minor texture within the microstructure. Furthermore the MRD values, which are determined by texture-related relative intensity changes in multiples of random distribution, are all low. The measured intensities are ranging between 0 and 2.7 MRD, while the calculated intensities are between 0.5 and 1.8 MRD, indicating the lack of significant texture (Figure 34).

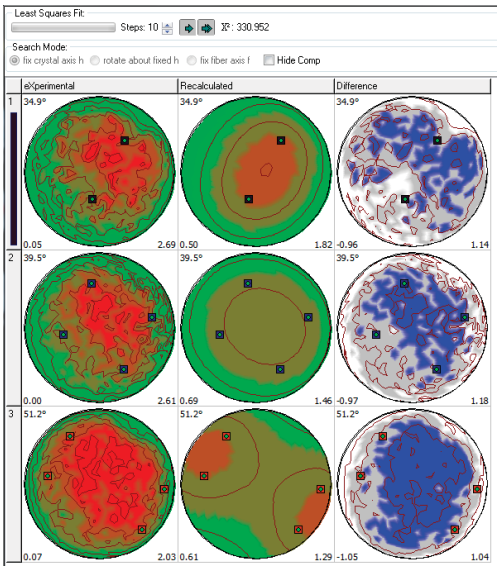

Figure 34. Measured and calculated pole figures of the α-uranium phase of U5Fs sample in (110) (top), (111) (center) and in (112) orientation (bottom).

The calculated pole figures for each orientation are displayed in Figure 35.

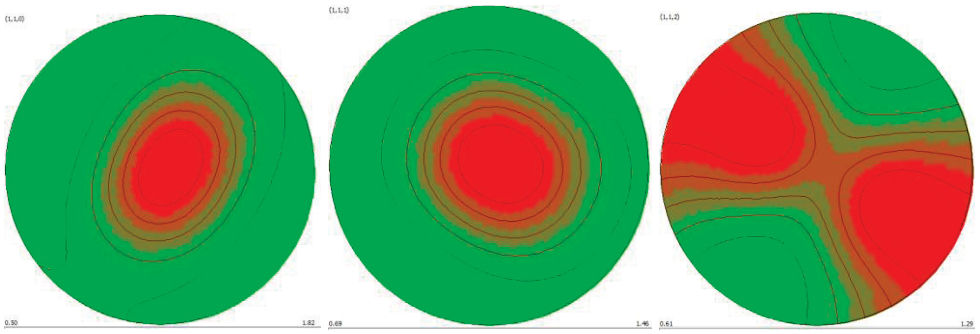

Figure 35. Calculated pole figures of the α-uranium phase of heat treated U5Fs.
Left: pole figure in (110) with MRD ranging from 0.5 to 1.8. Center: pole figure in (111) with MRD from 0.7 to 1.5. Right: pole figure in (112) with MRD from 0.6 to 1.3.

The inverse pole figures provide texture information in normal direction (ND), transverse direction (TD), and rolling direction (RD), and are displayed in Figure 36.

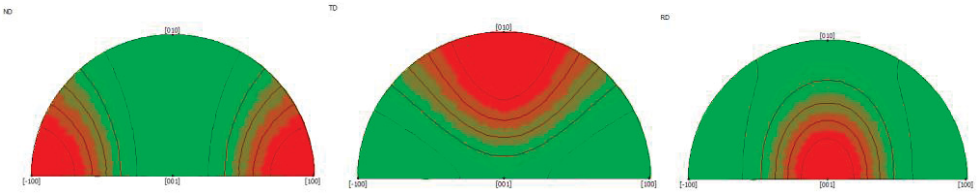

Figure 36. Calculated inverse pole figures of the α-uranium phase of heat treated U5Fs in normal direction (ND, top left), transverse direction (TD, top right) and rolling direction (RD, bottom).

Texture Analysis of the α-Uranium Phase in U5Fs using Peak Intensity Ratio Method

Qualitative texture analysis on cast EBR-II type fuel compositions were traditionally accomplished based on the approach published by Sturcken & Walter (JNM 50(1) (1974), 69-82). Hereby the relative peak intensity ratios $I_{(110)}/I_{(021)}$ were compared. These peak ratios indicate microstructural changes depending on the fuel fabrication process, e.g. from 0.8 (considered to be non-textured) for impact bonded to 1.3 for centrifugally bonded fuel pins, which were considered to be textured, creating anisotropic growth when irradiated or cycled thermally. Historically this method was applied to fuel containing only uranium, not to fuel containing both uranium and zirconium. While the U5Fs sample does not contain significant quantities of zirconium it does have contributions from other phases, mainly γ-uranium, which must be accounted for when applying the peak ratio method of analyzing texture. We have applied a similar approach to determine the intensity ratio $I_{(110)}/I_{(021)}$ in α-uranium phase of the bulk U5Fs sample using a combination of Rietveld refinement and Pawley-type peak fitting. Figure 37 shows the calculated α-uranium contribution to the overall U5Fs pattern.

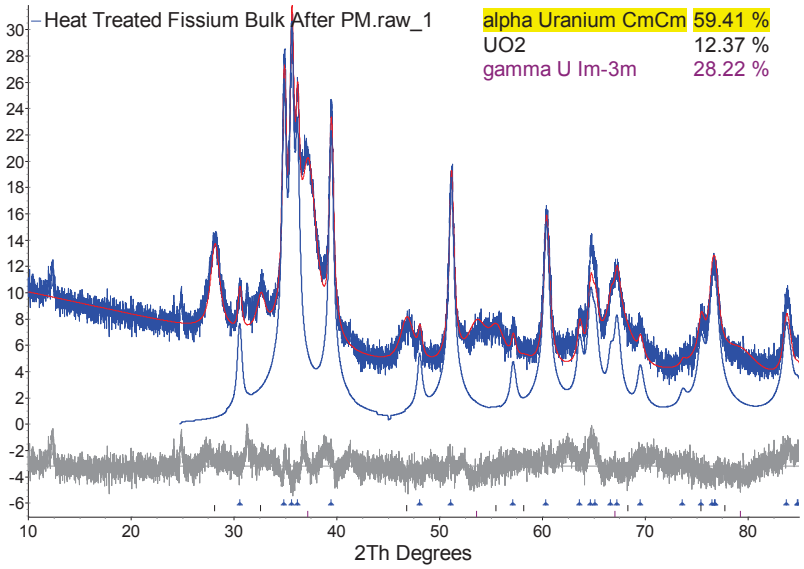

Figure 37. Rietveld structure refinement in the heat treated U5Fs sample.
The calculated α-uranium contribution is highlighted in blue.

The XRD pattern of U5Fs contains three major phases: α-uranium, γ-uranium and uranium dioxide and the refined lattice parameter and calculated phase content are listed in Table 4.

Table 4. Refined lattice parameter and phases content in U5Fs.

Phase	Lattice Parameter *a* [Å]	Lattice Parameter *b* [Å]	Lattice Parameter *c* [Å]	Contribution [wt.-%]
α-Uranium	2.8640 (3)	5.8501 (5)	4.9668 (4)	59.4 (± 0.4)
γ-Uranium	3.4178 (6)	*na*	*na*	12.4 (± 0.3)
UO_2	5.491 (1)	*na*	*na*	28.2 (± 0.4)

To overcome the impact of peak-peak overlay while applying the peak-ratio method based on Sturcken & Walter, we are now combining Rietveld structure refinement for the minor phases γ-uranium and UO_2 with Pawley fitting for α-uranium. For the Rietveld part the structure data for γ-uranium and uranium dioxide have to be considered texture-free. Pawley-fitting of the α-uranium "hkl phase" allows for an unconstrained fit of the diffracted intensities (Figure 38). This combination of Rietveld structure refinement and Pawley fitting for the α-uranium phase provides relative intensities as well as absolute peak intensities, and the peak intensity ratios $I_{(110)}/I_{(021)}$ are directly extracted with high accuracy.

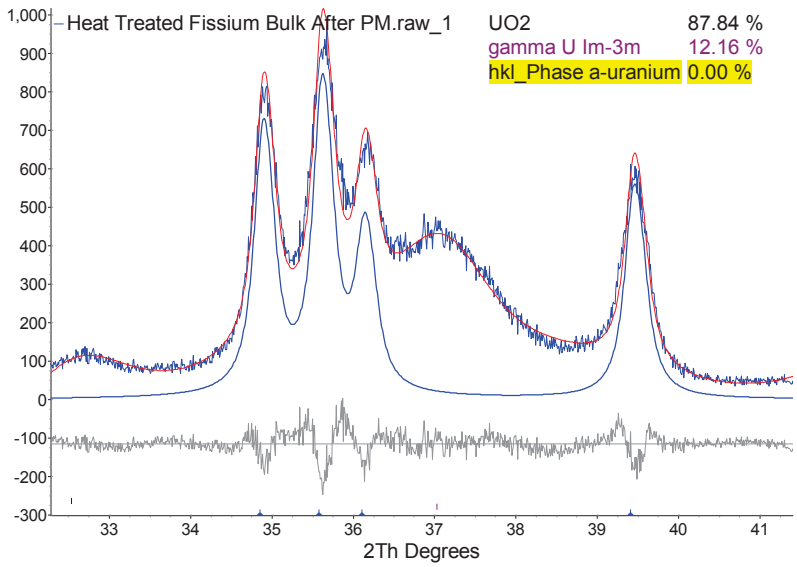

Figure 38. Refined XRD pattern of U5Fs.
The Pawley type fit for α-uranium is highlighted (blue pattern). **NOTE:** *A quantification of the hkl phase is not possible (structure amplitudes are not considered) and set to 0.*

The patterns of γ-uranium and uranium dioxide do slightly overlay with the pattern of α-uranium, but an exact quantification becomes possible assuming random orientation for γ-uranium and UO_2 (Figure 39).

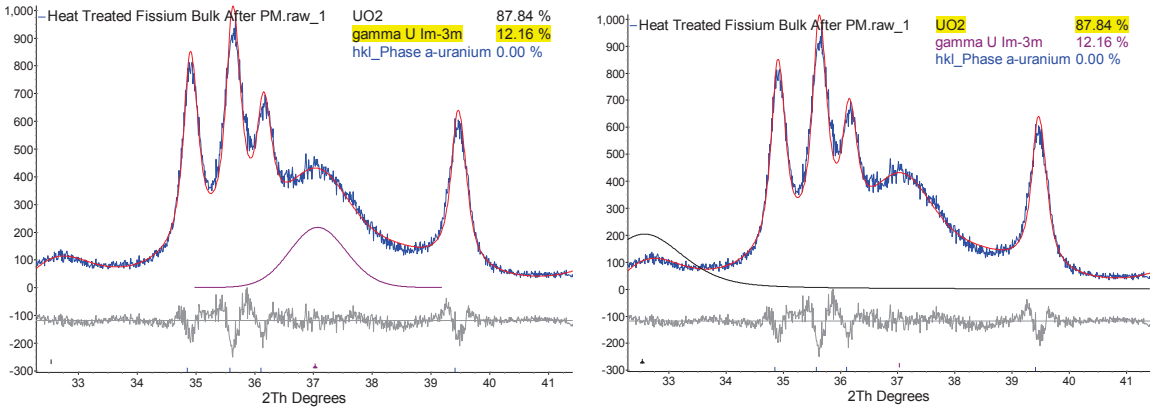

Figure 39. Peak overlay of α-uranium by γ-uranium (left) and uranium (right) with the assumption of random orientation for γ-uranium and uranium dioxide.

Based in these assumptions, the Pawley fit for α-uranium was successful to extract relative and absolute peak intensity ratios. The relative peak intensity ratio $I_{(110)}/I_{(021)}$ was measured to 0.862 (± 0.002) and the absolute peak intensity ratio $I_{(110)}/I_{(021)}$ to 0.833 (± 0.001). The 0.833 value falls within historical measurements and within the U5Fs fuel specification numbers of $0.74 < I_{(110)}/I_{(021)} < 0.84$ (L.C. Walters, G. L. Hofman and R.H. Rohde, trans. Am Nucl. Soc. V.17 (1973) p.217-218). Note however that the ratios using the test methods/equipment here are in general slightly less than the methods used previously. A perfectly random texture was considered to be 0.79 but a ratio of 0.738(2) for relative intensities and a $I_{(110)}/I_{(021)}$ ratio of 0.702(1) for absolute peak intensities is considered random using this experimental set-up. The ratio measured here is slightly higher than would be considered perfectly random.

Conclusion

XRD-based texture analysis using Multex 3 is successful in modeling texture in samples which have significant texture such as material processed e.g. by cold rolling or forging. The grains in the microstructure of such materials rearrange and the overall texture of the sample can be quantified straightforwardly. This is shown in the copper foil and the single crystal examples.

Unfortunately, the software has evident limitations in analyzing samples with relatively insignificant texture since small differences in the average crystallographic grain orientations compared to random grain distribution cannot be distinguished. In randomly or near randomly oriented samples changes in pole figures based on changed diffracted intensities cannot be clearly assigned to changes in crystallographic orientation. This is shown in the corundum pressed pellet example. Having a highly textured sample to compare with a random sample allowed us to explore the capabilities of the software. It also gave a comparison point for the samples of interest.

Due to the relatively low degree of texture in the fuel samples the software does not perform as well on these samples as it does on samples with a high degree of texture. If a microstructure is characterized by significant texture, XRD-based texture analysis using Multex 3 can be successfully applied to determine the structure model (spherical and/or fiber), crystallite orientation and the Euler angles, process-related changes of the sample symmetry (which is different than the crystallographic symmetry), and inverse pole figures relative to the normal direction (ND), the transverse direction (TD) and the rolling direction (RD). However, strong or insignificant texture can be distinguished by large and small MRD values, respectively, which describe diffracted intensity changes relative to a random distribution of the crystallites. MRD values are routinely used in texture analyses and are represented in the pole figures as an outcome of texture modeling using Multex 3. Below is a table of calculated and measured MRD values in the samples we report (Table 5).

Table 5. Measured and calculated MRD values for each sample analyzed

Sample	Measured MRD Value Range (background to pole)	Calculated MRD Value Range (background to pole)
Molybdenum Single Crystal	0 - 413	0 - 317
Cold-rolled Copper	0 - 12	0 - 8
Corundum (Al2O3) Pellet	0 - 3	0 - 1
α-Uranium	0 - 2	0 - 1
R1a2R1a5a (U10Zr)	0 - 5	0- 2
R1c2R1c5a (U10Zr)	0 - 3	0 - 1
R2c2R2c5a (U10Zr)	0 - 3	0 - 2
R2a2R2a5a (U10Zr)	0 - 3	0 - 2
Ra2Ra5a (U10Zr)	0 - 3	0 - 2
Heat Treated U5Fs	0 - 3	0 - 2

Table 5 summarizes the MRD values from baseline EBRII and FFTF radial fuel samples and the U5Fs sample. We used texture data from a molybdenum single crystal and a corundum pellet to determine both bounding conditions, for highest and lowest possible texture. Hereby we have established a broad data foundation and a good basis of texture data in support of future analysis to come. There is some concern that this technique might not be able to distinguish small amounts of texture in these

samples. The only way to test this would be to obtain a sample of the actual material of interest (U10Zr) that is known to have texture. If such a sample could be obtained we could better quantify the ability of this technique to determine texture in this material.

Path Forward

To support fuel production there is a need to have a method of quickly determining relative texture supported by the MRD technique. We have looked at the bulk data from the archived EBRII and FFTF fuel using the combination of Rietveld refinement and Pawley fitting for the α-uranium phase. This method assumes that the UZr_2 phase is randomly oriented. From this analysis it has been determined that a slower bulk run will be required on the samples in order to gather a sufficient quantity of data to test the Pawley fitting method

In order to verify that the pole figure (MRD) and Pawley fitting techniques, also called peak height ratio (PHR), would both equivalently detect texture we will conduct a series of MRD and Peak Height Ratio (PHR) analyses on samples from extruded, or rolled, and cast uranium. Rolling would be used as an alternative to extrusion to texture uranium and U10Zr samples for these additional analyses . A test matrix identifying the number of samples along with extrusion/rolling temperatures and reduction ratios will be developed to track and report the progress of the analyses.